Cerebral Cortex August 2012;22:1799–1812
doi:10.1093/cercor/bhr258
Advance Access publication September 22, 2011

Androgen Influence on Prefrontal Dopamine Systems in Adult Male Rats: Localization of Cognate Intracellular Receptors in Medial Prefrontal Projections to the Ventral Tegmental Area and Effects of Gonadectomy and Hormone Replacement on Glutamate-Stimulated Extracellular Dopamine Level

T. Aubele[1,2,3] and M. F. Kritzer[2]

[1]Graduate Program in Neuroscience and [2]Department of Neurobiology and Behavior, Stony Brook University, Stony Brook, NY 11794-5230, USA and [3]Department of Psychology, Florida State University, Tallahassee, FL 32306-4301, USA

Address correspondence to Teresa Aubele, Department of Psychology, Florida State University, Tallahassee, FL 32306-4301, USA.
Email: aubele@psy.fsu.edu.

Although androgens are known to modulate dopamine (DA) systems and DA-dependent behaviors of the male prefrontal cortex (PFC), how this occurs remains unclear. Because relatively few ventral tegmental area (VTA) mesoprefrontal DA neurons contain intracellular androgen receptors (ARs), studies presented here combined retrograde tracing and immunolabeling for AR in male rats to determine whether projections afferent to the VTA might be more AR enriched. Results revealed PFC-to-VTA projections to be substantially AR enriched. Because these projections modulate VTA DA cell firing and PFC DA levels, influence over this pathway could be means whereby androgens modulate PFC DA. To assess the hormone sensitivity of glutamate stimulation of PFC DA tone, additional studies utilized microdialysis/reverse dialysis application of α-amino-3-hydroxy-5-methyl-4-isoxazolepropionic acid and *N*-methyl-D-aspartate receptor subtype-selective antagonists which act locally within the PFC and tegmentally via inhibition or disinhibition of PFC-to-VTA afferents to modulate intracortical DA levels. Here, we compared the effects of these drug challenges in control, gonadectomized, and gonadectomized rats given testosterone or estradiol. This revealed complex effects of gonadectomy on antagonist-stimulated PFC DA levels that together with the anatomical data above suggest that androgen stimulation of PFC DA systems does engage glutamatergic circuitry and perhaps that of the AR-enriched glutamatergic projections from PFC-to-VTA specifically.

Keywords: AMPA, immunohistochemistry, microdialysis, NMDA, schizophrenia

Introduction

The prefrontal cortices (PFC) mediate highest order cognitive, executive, and mnemonic functions (Goldman-Rakic et al. 1990; Dalley et al. 2004) and are implicated in some of the most debilitating forms of cognitive dysfunction known in mental illness, including that seen in schizophrenia (Egan et al. 2001; Goldberg et al. 2003; Winterer and Weinberger 2004). Studies in humans and animal models have shown that in both males and females, gonadal hormones are capable of modulating PFC function and may also influence its dysfunction in disease (van Haaren et al. 1990; Janowsky et al. 2000; Luine 2008). In males, androgens appear to have particular potency in these modulatory roles. For example, significant direct correlations have been identified between circulating testosterone levels and performance in PFC-dependent tasks in healthy adult and aged men (Cherrier et al. 2001, 2007). There have also been correlations between hormone titers and performance on these same tasks in males with hormone abnormalities, for example, Klinefelter's syndrome, prostate cancer patients undergoing androgen deprivation therapies (Patwardhan et al. 2000; Cherrier et al. 2001; Janowsky 2006; Cherrier et al. 2007; Nelson et al. 2007) and in males diagnosed with disorders where PFC operations are especially at risk, including schizophrenia (Shirayama et al. 2002; Goyal et al. 2004; Taherianfard and Shariaty 2004; Akhondzadeh et al. 2006; Janowsky 2006; Ko et al. 2007; Nelson et al. 2007). Importantly, the roles for androgens implicit in these correlations have also been corroborated in animal models. In adult male rats, for example, gonadectomy (GDX) has been shown to impair, and androgen but not estrogen replacement restore, PFC-dependent processes including spatial working memory and behavioral flexibility (Adler et al. 1999; Ceccarelli et al. 2001; Daniel et al. 2003; Sandstrom et al. 2006; Kritzer et al. 2007; Aubele et al. 2008; Gibbs and Johnson 2008). Furthermore, androgen's impact on PFC operations seems to be related to its regulation of the PFC's functionally essential dopamine (DA) innervation. For example, in addition to affecting PFC behaviors that are known to be DA sensitive (Tassin et al. 1978; Kessler and Markowitsch 1981; Stam et al. 1989; Murphy et al. 1996; Zahrt et al. 1997; Morrow et al. 2000), GDX has also been shown to significantly elevate, and androgen but not estrogen replacement to restore, DA axon density and resting extracellular DA levels within the PFC (Kritzer et al. 1999; Kritzer 2000, 2003; Aubele and Kritzer 2011).

While androgen stimulation of PFC DA systems is likely to be important in androgen's influence over PFC function, recent studies have shown that fewer than one quarter of the mesoprefrontally projecting DA cells of the ventral tegmental area (VTA) contain intracellular androgen receptors (ARs)—the receptive machinery required for genomic androgen action (Kritzer and Creutz 2008). This modest proportion makes it unlikely that direct stimulation of mesoprefrontal DA cells within the VTA is the major means by which androgen influences PFC DA systems. Accordingly, the first series of studies presented here combined tract tracing and immunostaining for AR to determine whether pathways that are afferent to the VTA might instead be sites of more substantial androgen influence. These analyses revealed the unexpected finding that of all of the major afferent projections to the VTA, those arising from pyramidal cells of the PFC itself were by far the most AR enriched. These projections are well known to regulate cell firing of DA neurons in the VTA and in turn DA levels in the PFC (Gariano and Groves

1988; Gonon 1988; Overton and Clark 1997; Schultz 1998) and are key parts of glutamate hypotheses of PFC function and of its dysfunction in schizophrenia and other disorders (Moghaddam 2003; Lewis and Moghaddam 2006; Javitt 2007; Arnsten 2009; Scott and Aperia 2009; Seeman 2009; Javitt 2010; Marek et al. 2010). To begin to explore the question that these anatomical observations raise regarding hormone influence over glutamate stimulation of PFC DA tone, selective α-amino-3-hydroxy-5-methyl-4-isoxazolepropionic acid (AMPA) and *N*-methyl-D-aspartate (NMDA) glutamate receptor antagonists were applied via reverse dialysis to the PFC of gonadally intact, GDX, and GDX rats supplemented with estradiol or testosterone propionate. These antagonist challenges are thought to act both locally within the PFC as well as at the tegmental level via inhibition and disinhibition the PFC's corticofugal connections to the VTA with end results of decreasing and increasing extracellular PFC DA levels, respectively (Feenstra et al. 1995; Jedema and Moghddam 1996; Verma and Moghaddam 1996; Moghaddam et al. 1997; Takahata and Moghaddam 1998; Feenstra et al. 2002). Using HPLC with electrochemical detection (HPLC-EC) to measure PFC DA concentration, the effects of these established glutamate receptor antagonist challenge paradigms to lower and raise extracellular DA levels in the PFC were quantitatively compared across hormone treatment groups.

Materials and Methods

Animal Subjects

A total of 43 adult male Sprague–Dawley rats (Taconic Farms, Germantown, NY) were used. Animals were housed in pairs of like treatment under a 12/12 h light/dark cycle (lights on at 0700) with food (Purina PMI LabDiet: Prolab RMH 3000) and water available ad libitum. Five gonadally intact rats were used for the tract-tracing studies. Of the remaining animals, 10 served as sham operated (CTRL), 10 were gonadectomized (GDX), 10 were GDX and supplemented with testosterone propionate (GDX-TP), and 8 were GDX and supplemented with 17-β-estradiol (GDX-E). Among these 4 groups, half of the subjects were used in microdialysis experiments in which the NMDA antagonist D(−)-2-amino-5-phosphonopentanoic acid (APV) was administered and half were used in experiments in which the AMPA antagonist 2, 3-dihydroxy-6-nitro-7-sulfamoyl-benzo[f]quinoxaline-2,3-dione (NBQX) was given. All procedures involving animals were approved by the Institutional Animal Care and Use Committee at Stony Brook University and were designed to minimize animal use and discomfort.

Surgeries

All surgeries were carried out aseptically using intraperitoneal injections of ketamine (0.9 mg/kg) and xylazine (0.5 mg/kg) as anesthesia, with 0.03 mg/kg buprenorphine administered to manage postoperative discomfort.

Stereotaxic Injection of Retrograde Tracer

Ten days prior to euthanasia, gonadally intact rats were anesthetized and placed in a stereotaxic frame (Kopf Instruments, Tujunga, CA). Incisions were made to expose the skull and burr holes were drilled. Glass micropipettes containing the retrograde tracer cholera toxin (β subunit, conjugated to 7 nm colloidal gold, List Biologicals, Campbell, CA) diluted to 0.025% in sterile water were inserted and lowered into the left VTA, and ~50 nL of tracer was then slowly pressure injected in 5–15 nL increments over a 30-min period. Afterward, pipettes were left in place for 15 min before being slowly withdrawn. Burr holes were packed with sterile gel foam and incisions were closed using prolene sutures.

Gonadectomy, Sham Surgery, and Hormone Replacement

Twenty-eight days before microdialysis experiments, rats were anesthetized and GDX or sham surgery was performed. For both procedures, the sac of the scrotum and the underlying layers of tunica were incised. For GDX, the vas deferens was also bilaterally ligated using sterile nonabsorbable silk sutures and the testes were removed. For the hormone replacement groups, pellets that released testosterone propionate (TP, GDX-TP rats) or 17β-estradiol (E, GDX-E rats, Innovative Research of America, Sarasota, FL) were inserted within the tunica (see below). Following surgery, incisions through the scrotum and tunica were closed using sterile wound clips that were removed 2 weeks after surgery.

Stereotaxic Placement of Guide Cannulae

Twenty-four hours before microdialysis experiments, CTRL, GDX, GDX-E, and GDT-TP rats were anesthetized and craniotomies were performed (above) to place guide cannulae (CMA Microdialysis, North Chelmsford, MA) over the left pregenual medial PFC (mPFC). Cannulae were secured to the skull using shallow screws and dental cement.

Hormone Treatment and Validation

Gonadectomized rats received 60-day slow release pellets (Innovative Research of America) that contained either TP or E in biodegradable matrix. The TP-containing pellets released approximately 3–4 ng of TP per milliliter of blood per day, and the E-containing pellets released approximately 25 pg of 17-β-estradiol per milliliter of blood per day. Both have been used in previous investigations in this laboratory and others and have been shown to maintain circulating plasma levels of gonadal hormones in gonadectomized rats within physiological ranges (Collins et al. 1992; Adler et al. 1999; Kritzer 2000). Their efficacy in this study was verified in quantitative group comparisons of the weights of animals' androgen-sensitive bulbospongiosus muscles (BSMs) (Wainman and Shipounoff 1941) and of resting extracellular PFC DA concentrations (Aubele and Kritzer 2011).

In Vivo Microdialysis and HPLC/EC Analysis

Dialysate samples were collected during the rats' subjective night and were directly injected into an HPLC system (PM 92-E pump, BAS, West Lafayette, IN) via an online autoinjector (Pollen-8, BAS). Analyses utilized a microbore column (UniJet, 1.0 mm inner diameter, 150 mm length, 5 μm Octadecylsilane particles; BAS) and a BioAnalytical Systems LC-Epsilon detector (BAS). The E_{app} was + 0.65 V versus the Ag/AgCl reference electrode. The mobile phase consisted of 14.5 mM NaH_2PO_4; 30 mM sodium citrate; 10 mM diethylamine HCl; 2.2 mM 1-octanesulfonic acid; 0.027 mM ethylenediaminetetraacetic acid; 7.2% acetonitrile (v/v); 1% tetrahydrofuran (v/v), pH 3.4. Probe efficiency was determined to be 10–18% for all studies, and an overall detection limit of 8 fmol was achieved. All chemicals used were purchased from Sigma-Aldrich Chemical Co. (St Louis, MO).

One day after guide cannulae were implanted, rats were placed in Raturn clear rodent bowls (BioAnalytical Systems) for a 10-min acclimation period. Afterward, microdialysis probes (100,000 Da cutoff, 3 mm PES exposed membrane tip, CMA Microdialysis) were inserted through the guide cannulae and perfused for 2 h with artificial cerebrospinal fluid (CSF) (145 mM NaCl; 2.8 mM KCl; 1.2 mM $MgCl_2$, 0.25 mM ascorbic acid; 5.4 mM D-Glucose, 1.2 mM $CaCl_2$ in 1L H_2O, pH 6.8, flow rate of 2 μL/min). Baseline dialysates were then collected at the same flow rate and injected into the HPLC system every 20 min. After collection of 3 successive samples with stable DA levels, drug delivery was initiated. Either 500 μM APV (Sigma Chemical Co.) or 150 μM NBQX (Sigma Chemical Co.) dissolved in artificial CSF was delivered via reverse dialysis for 120 min. Dialysate samples were collected every 20 min during the drug delivery period and thereafter until PFC DA levels returned to stable predrug baseline values for 3 successive samples.

Euthanasia

Animals that had been injected with retrograde tracer were deeply anesthetized with ketamine and xylazine (90 and 10 mg/kg, respectively) and were transcardially perfused with phosphate buffered saline, pH 7.4, followed by 800 mL of 0.1 M phosphate buffer (PB), pH 7.4, containing 2% paraformaldehyde and 15% picric acid (flow rate of 30 mL/min) 10 days after surgery. Afterward, brains were removed and

postfixed in the same fixative solution for 1 h at room temperature. Next, the brains were cryoprotected in 30% sucrose in 0.1 M PB and were rapidly frozen in powdered dry ice. Rats used in microdialysis studies were euthanized after the experiments by rapid decapitation; their brains were removed, postfixed, and cryoprotected in a 30% sucrose, 10% buffered formaldehyde solution and rapidly frozen in powdered dry ice. The androgen-sensitive medial, ventral, and lateral BSMs from these animals were also dissected out and weighed.

Histology

All brains were serially sectioned in the coronal plane on a freezing microtome (40 μm). Prior to histology, sections were stored in cryoprotectant buffer (30% glycerol (v/v), 30% ethylene glycol (v/v) in 0.01 M PB) at −20 °C.

VTA Injection Sites

"VTA injection sites" were evaluated in 1 in 3 series of sections through the ventral midbrain and retrograde labeling was assessed in 1 in 6 series of sections through the rest of the brain. In both cases, the gold-conjugated cholera toxin tracer was revealed by a silver-plating reaction. Briefly, free-floating sections were rinsed in 0.1 M PB, pH 7.4 (4 × 15 min), incubated in IntenSE silver enhancement solution (4 × 30 min; GE Healthcare Life Sciences), rinsed again in 0.1 M PB, and fixed in 2.5% sodium thiosulfate (10 min). Injection site boundaries and retrograde labeling were mapped in slide-mounted sections that were counterstained with 0.5% cresyl violet to reveal cytoarchitecture. Only those cases where injection sites were confined to the left rostroventral VTA (Fig. 1*A*,*D*–*F*) and where patterns of retrograde labeling were similar to those described in previous tract-tracing studies (Phillipson 1978; Geisler and Zahm 2005) were used in the analysis.

Dual Visualization of Retrograde Labeling and Immunocytochemistry

"Dual visualization of retrograde labeling and immunocytochemistry for AR" was achieved using a double-labeling protocol in which sections were first incubated in 1% H_2O_2 in 0.1 M PB (40 min) and then silver enhanced as above. Afterward, sections were rinsed in Tris-buffered saline (TBS), pH 7.4 (3 × 15 min), blocked in 10% normal swine serum (NSS) in TBS (2 h, room temperature), and placed in primary antisera (anti-AR, rabbit polyclonal, Millipore, catalog no. 06-680, lot no. 33529; antigen-synthetic peptide, 21 amino acid N-terminal sequence of human ARs, working dilution 1:1000) diluted in TBS containing 10% NSS. After incubation for 4 days (4 °C), sections were rinsed in TBS and placed in biotinylated secondary antibodies (Vector Laboratories, Temecula, CA, working dilution 1:100) for 2 h at room temperature. After further rinsing in TBS, sections were incubated in avidin-conjugated horseradish peroxidase solution (ABC [avidin–biotin complex] kit, Vector Laboratories) for 2 h at room temperature, rinsed again in TBS, and then in TB. The tissue was then reacted using 3,3′-diaminobenzidine (DAB)–nickel solution (0.014% DAB and 0.6% nickel ammonium sulfate in TB, pH 8.0) as chromagen. Control experiments assessed the specificity of the commercially available anti-AR antibody used in representative fore- and hindbrain sections by using the immunolabeling protocol described above (in combination with silver intensification) performed with omission of primary or secondary antisera. Only those cases where immunoreactivity for AR (AR-IR) showed clear nuclear signal and conformed to expected patterns of localization and apparent densities (Simerly et al. 1990; Hamson et al. 2004; DonCarlos et al. 2006; Feng et al. 2010) were used in the analysis.

Microdialysis Probe Placement

"Microdialysis probe placement" was evaluated from a 1 in 4 series of sections taken from midolfactory bulb through the genu of the corpus callosum that were slide mounted and stained with 0.5% cresyl violet. Light microscopic evaluation was used to map probe locations with respect to cortical cytoarchitecture. In order for data from a given subject to be included in the analysis, probes had to have been placed in the left pregenual mPFC, extend dorsoventrally through prelimbic and infralimbic areas but not beyond, and be centered over middle and deep cortical layers (Fig. 1*A*,*B*).

Data Analysis

Tract Tracing/Immunocytochemistry

The distributions and AR immunoreactivity of retrogradely labeled cell populations were assessed by a single observer (T.A.). Using a Zeiss Axioskope microscope fitted with a camera lucida, low-power objectives (10×) and dark-field optics were used to plot regional patterns of retrograde labeling and AR-IR among cytoarchitectonically identified regions of interest. High-power objectives (40×) and bright-field optics were used to assess the incidence of double labeling within identified regions on cell-by-cell bases. Uncorrected counts were made of all visible singly (retrograde tracer) and doubly (retrograde tracer +

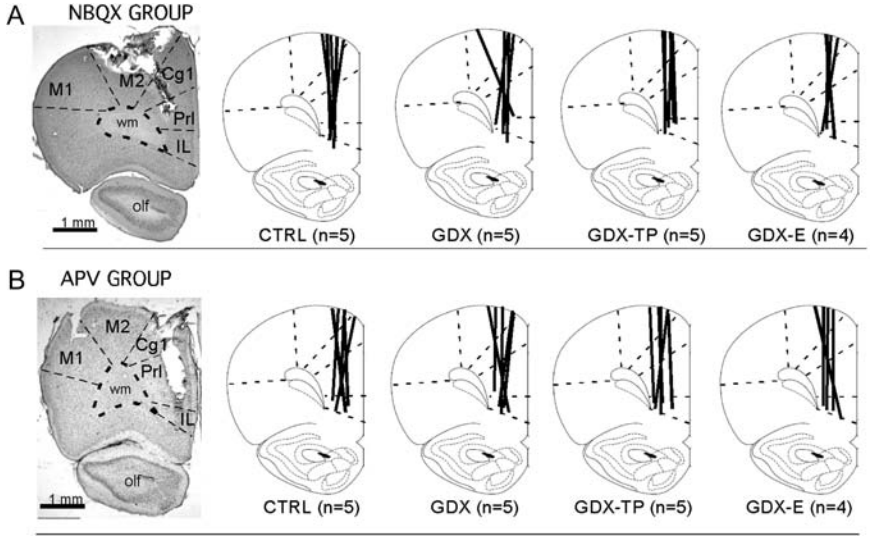

Figure 1. Representative low-power photomicrographs showing the track of a microdialysis probe in cresyl violet counterstained sections of the mPFC of control animals from the NBQX (*A*) and the APV (*B*) studies. The boundaries between cytoarchitectonic areas and between cortex and white matter are marked with dashed lines. Line drawings (modified from Paxinos and Watson 1998) to the right depict the locations of microdialysis probe tracks (thick black lines) for each sham-operated control (CTRL), gonadectomized (GDX), and gonadectomized rats supplemented with testosterone propionate (GDX-TP) or 17-β-estradiol (GDX-E) used in the NBQX (*A*) or APV (*B*) study. The numbers that appear in parentheses below the drawings correspond to the number of animal subjects in that group. Abbreviations: Cg1, anterior cingulate cortex; IL, infralimbic cortex M1, primary motor cortex; M2, premotor cortex; olf, olfactory nuclei and tract; PrL, prelimbic cortex.

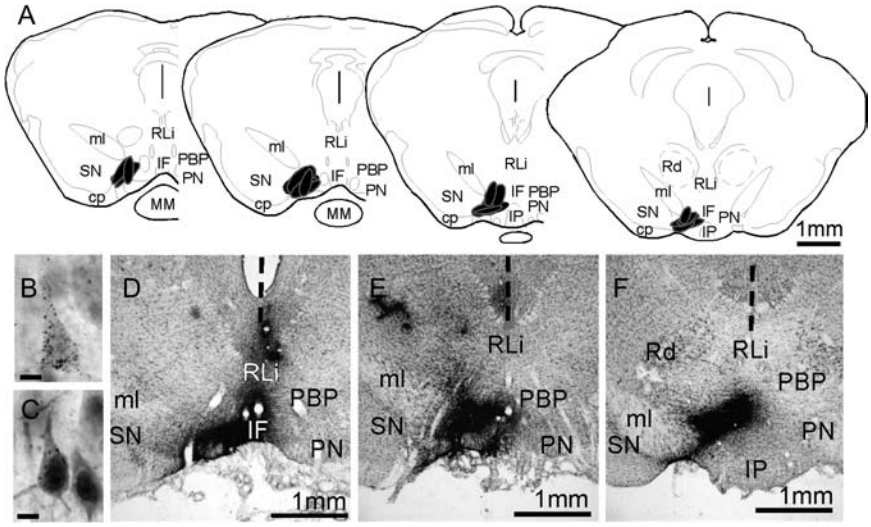

Figure 2. (*A*) Schematic maps showing the locations of VTA injection sites from the 5 animal subjects used in this study. The section outlines shown are adapted from the atlas of Paxinos and Watson (1998) and the locations of injection sites are shown in black. Low-power photomicrographs (*D–F*) show that injection sites appear in situ as dense, blackened areas; these were localized with respect ventral midbrain cytoarchitecture in 1 in 3 series of 40 μm cresyl violet stained sections (*D–F*). The vertical dashed line in these images marks the midline. High-power photomicrographs (*B*,*C*) show the appearance of representative neurons that are retrogradely labeled by the gold-conjugated cholera toxin injections. The cytoplasm of both pyramidal cells contains above background levels of silver-enhanced gold particles; the retrogradely labeled cell shown in *C* also shows nuclear localization of immunoreactivity for intracellular AR and is situated next to a cell that is immunoreactive for AR but that is not retrogradely labeled. Abbreviations: cp, cerebral peduncle; IF, interfascicular nucleus; IP, interpeduncular nucleus; ml, medial lemniscus; MM, mammillary nucleus; PBP, parabrachial VTA; PN, paranigral VTA; Rd, red nucleus; RLi, rostrolinear nucleus; SN, substantianigra. Scale bars in *B*,*C* = 10 microns.

AR-IR) labeled cells within defined rectangular counting fields (below) whose boundaries were superimposed via camera lucida over the images of the tissue section. Singly labeled cells occurring within these frames were defined as those containing above background levels of silver grains within the cytoplasm (Fig. 2*B*) and double-labeled cells were defined as those that additionally contained a nucleus that had above background levels of blue–black DAB–nickel reaction product (Fig. 2*C*). For inclusion in counting, both singly and doubly labeled cells had to have a visible nucleus.

In each animal subject, the percentages of all visible retrogradely labeled cells meeting inclusion criteria that were also AR-IR were calculated on per-structure and per-hemisphere bases from at least 3 nonoverlapping 257 × 425 μm counting frames that were optically superimposed (camera lucida) over the labeled field within the cytoarchitectonically defined region of interest; the upper and right-hand sides of these frames served as exclusion lines. Every brain region included in the analysis contained 50–600 countable, back-labeled cells per region, per hemisphere, per animal. Because the olfactory tubercle, magnocellular preoptic area, and pedunculopontine nucleus contained fewer than 30 total cells meeting inclusion criteria per hemisphere per animal, no attempts were made to quantify double labeling in these sparsely areas.

Microdialysis: DA Concentration

DA peaks were identified and quantified (ng/10 mL) in relation to standards of known DA concentration (1, 2, 5, 10 ng/10 mL) run through the HPLC system on the same day that the animal's data were collected; uncorrected peak values were measured automatically by ChromGraph software (BAS) as "peak height" and were converted to concentrations (fmol/μL) using the standards. Predrug DA baseline collection was considered complete once 3 consecutive stable measurements were obtained prior to drug onset; drug-induced changes in DA levels were quantified both as percent of predrug baseline and as absolute DA concentration (fmol/μL); DA levels were defined as returning to baseline in the postdrug period when 3 successive stable measures were obtained that did not significantly differ from predrug DA values.

Statistics

DA concentration data were initially evaluated using 2-way mixed-model analyses of variance (ANOVAs) with repeated measured designs, with the 20 min sample bins serving as a within-subjects factor and group (CTRL, GDX, GDX-TP, GDX-E) serving as a between subjects factor. These analyses were used to identify significant main effects of hormone treatment on drug-induced changes in PFC DA level. Subsequent analyses included within-groups assessments of the effect of time on DA concentration. First, 1-way ANOVAs with repeated measures design, with DA level from each of the 20 min samples serving as within-subjects factors, were run and allowed post hoc tests (Fisher's Protected Least Significant Difference, PLSD) further identified significant differences in DA level as occurring among individual samples collected before, during, or after drug application. Finally, DA concentration from corresponding 20 min bin samples were also compared across groups in 1-way ANOVAs that were followed by post hoc tests (PLSD) to determine where along the course of drug delivery effects on DA concentration differed among the hormone treatment groups. All ANOVA assessments were preceded by Levine's *F*-test for equality of variance and Mauchly's sphericity test to ensure that observations obeyed all required assumptions. A Greenhouse–Geisser correction was applied as necessary. In all cases, $P < 0.05$ was accepted as significant and $0.05 < P < 0.09$ was identified as near significant. BSM weights were also compared across groups using regular 1-way ANOVAs.

Results

Localization of Immunoreactivity for Intracellular ARs in Neurons Projecting to the VTA

The question of whether neurons making afferent projections to the VTA were AR-IR was addressed in gonadally intact adult male rats. All animals included in the analyses had injection sites of the retrograde tracer cholera toxin (β subunit) localized to similar areas within the left rostral VTA (Fig 2*A*,*D–F*). The distributions of neurons retrogradely labeled by these VTA injection sites were similar in all animals evaluated and to similar results described in previous retrograde tracing studies in rats (Phillipson 1978; Geisler and Zahm 2005). For example, labeling was bilateral, albeit more dense ipsilateral to injection sites and

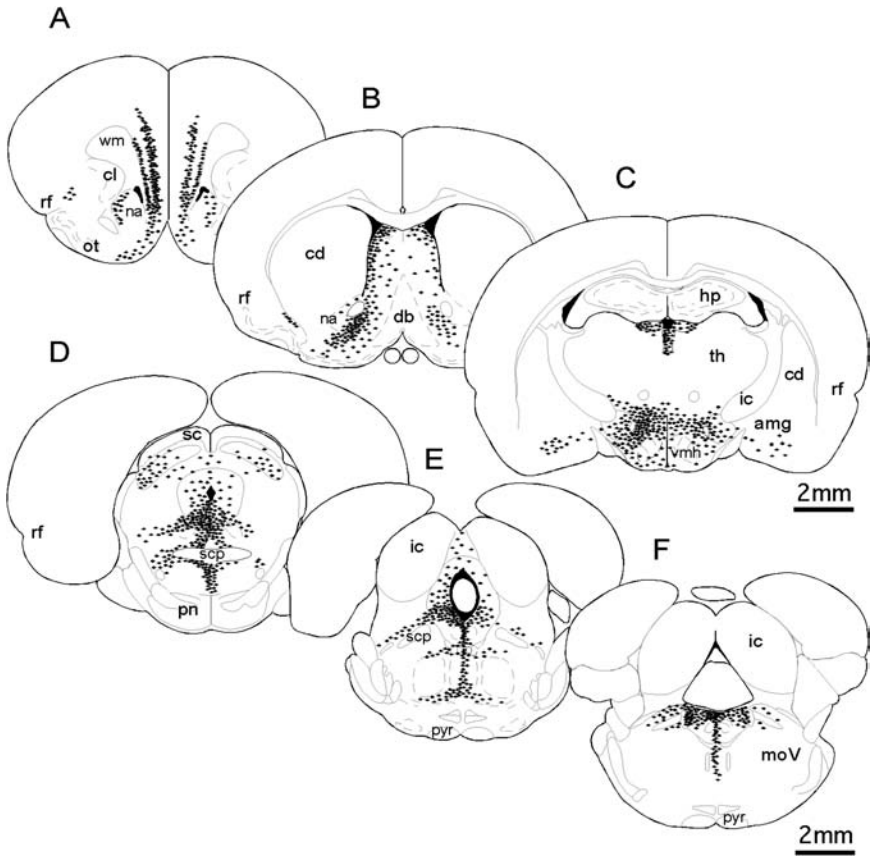

Figure 3. Schematic diagrams derived from camera lucida drawings representing the distribution and relative density of neurons (black symbols) retrogradely labeled by cholera toxin injections localized to the VTA rostral (*A–C*) and caudal (*D–F*) to the injection site level. Each black symbol shown represents 3–5 back-labeled cells; section outlines are adapted from Paxinos and Watson (1998). Similar to what has been described previously, cells that project to the VTA are located bilaterally and tend to be clustered among structures that are ventral and lateral to the midline from the level of the pregenual PFC (*A*) to midmedulla (*F*). Labeling is also noticeably more dense in hemispheres ipsilateral to injection sites (left-hand side). Abbreviations: amg, amygdala; cd, caudate nucleus; cl, claustrum; db, diagonal band; ic, inferior colliculus; hp, hippocampus; internal capsule; moV, motor trigeminal nucleus; nucleus accumbens; ot, olfactory tubercle; pn, pontine nuclei; pyr, pyramidal tract; rf, rhinal fissure; sc, superior colliculus; scp, superior cerebellar peduncle; th, thalamus; vhm, ventromedial hypothalamus.

was clustered within a loosely organized medial to ventromedial continuum that extended from the rostral PFC to midmedullary levels (Fig. 3*A–F*). The regional and cellular distributions of AR immunoreactivity were also similar in all of the animals evaluated and were comparable to patterns of labeling described in previous immunocytochemical and in situ hybridization studies (Simerly et al. 1990; Hamson et al. 2004; DonCarlos et al. 2006; Feng et al. 2010). Thus, immunolabeling was predominantly nuclear with lighter but still above background levels of labeling often seen in the surrounding cytoplasm (Figs 1*C* and 4*A*,*B*), was widespread, and was particularly dense among hypothalamic and preoptic nuclei (Fig. 4*E*), in parts of the amygdala and thalamus (Fig. 4*D*), along the midline in and around the septal nuclei and periaqueductal gray (Fig. 4*F*), and in the hippocampus and cerebral cortex (Fig. 4*C*).

Every brain area that was retrogradely labeled by VTA injections also contained at least moderate levels of AR immunoreactivity. However, in most of the areas examined, the proportions of retrogradely labeled cells that were also AR-IR was extremely low (Table 1). This was true for all back-labeled subcortical structures where, for 11 of the 22 separate areas assessed, including regions such as the medial preoptic area and bed nucleus of the stria terminalis where both retrograde labeling and receptor immunoreactivity were prominent, fewer than 2% of the several hundred back-labeled cells evaluated per region, per hemisphere, per animal were also AR-IR (Table 1). For most of the remaining retrogradely labeled subcortical fields, AR-IR cells accounted for less than 20% of all back-labeled cells and in only 2 subcortical regions—the dorsal raphe and locus coeruleus—did the incidence of AR-IR/cholera toxin double labeling rise slightly higher to account for 25–35% of all retrogradely labeled cells (Table 1). In the cerebral cortex, however, the proportions of retrogradely labeled cells that were also AR-IR were considerably higher (Table 1). Specifically, in each of the 3 retrogradely pregenual PFC fields (IL, PrL, Cg1), more than one-third of all back-labeled cells present in layer VI (both hemispheres), roughly 50–60% of all back-labeled cells present in V in the ipsilateral hemisphere, and some 40–50% of all tracer-labeled cells present in layer V in the contralateral hemisphere were also AR-IR (Table 1 and Fig. 5). These percentages are the highest for any projection from any brain area to the VTA and are markedly higher than the proportions of mesoprefrontal DA cells that are AR-IR.

Effects of GDX and Hormone Replacement on the Ability of PFC Application of AMPA and NMDA Antagonists to Modulate Extracellular DA Levels

To investigate whether glutamatergic circuitry might be engaged in androgen's regulation of PFC DA levels, local reverse dialysis infusion of glutamate receptor subtype-selective antagonists into the PFC were coupled with comparative microdialysis/HPLC

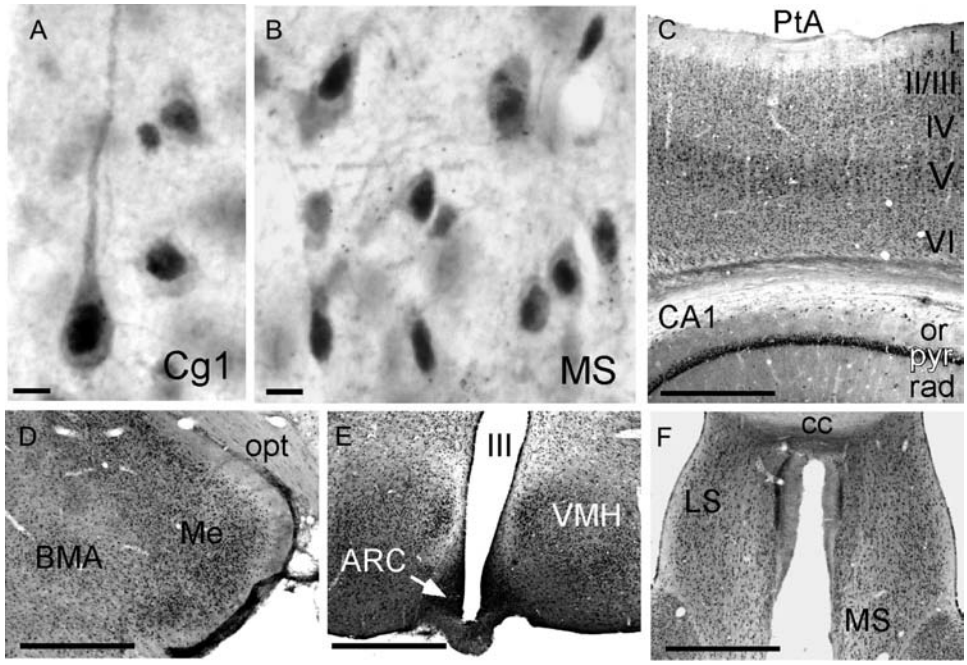

Figure 4. (*A*,*B*) High-power photomicrographs showing the cellular distribution of immunoreactivity for intracellular AR. The dense nuclear and lighter cytoplasmic signal that identify immunopositive cells can be seen in representative pyramidal cells from anterior cingulate (Cg1) cortex (*A*) and multipolar cells from the medial septal nucleus (MS, *B*). (*C*–*F*). Lower power photomicrographs illustrate expected patterns of AR-immunoreactive cells, visible as small black dots, which are especially dense in the pyramidal cell layers of cerebral (II/III, V, VI) and hippocampal cortex (pyr, *C*), within the medial nucleus of the amygdala (Me, *D*), the arcuate (ACR), and ventromedial hypothalamic nuclei (VMH, *E*), and in the medial (MS) and lateral (LS) septal areas (*F*). Other abbreviations: BMA, basomedial nucleus of the amygdala; cc, corpus callosum; op, optic tract; or, stratum oriens; PtA, parietal cortex; rad, stratum radiatum; III, third ventricle. Scale bars *A*,*B* = 20 microns; scale bars *C*–*F* = 1 mm.

Table 1

Mean percentage (±standard error of the mean) of all visible cells that were retrogradely labeled by injections of cholera toxin B-subunit into in the VTA which met inclusion criteria (visible nucleus) and were also immunoreactive for intracellular AR

Subcortical area	Ipsilateral	Contralateral
Amygdala	<2%	<2%
Bed nucleus of the stria terminalis	<2%	<2%
Claustrum	<2%	<2%
Medial preoptic area	<2%	<2%
Medial septal nuclei	<2%	<2%
Nucleus accumbens shell	<2%	<2%
Retrorubral fields	<2%	<2%
Supramammillary nucleus	<2%	<2%
Tuber cinereum	<2%	<2%
Ventral pallidum	<2%	<2%
Zona incerta	<2%	<2%
Superior colliculus	2.67 ± 0.16%	3.76 ± 0.43%
Median raphe nucleus	7.38 ± 0.80%	<2%
Medial habenula	9.49 ± 1.09%	8.46 ± 1.93%
Lateral preoptic area	15.89 ± 1.11%	18.77 ± 3.43%
Lateral hypothalamus	16.13 ± 1.84%	16.51 ± 2.15%
Lateral habenula	16.78 ± 1.19%	16.54 ± 2.80%
Lateral septal nuclei	17.92 ± 1.23%	24.92 ± 3.64%
Lateral dorsal tegmental nucleus	20.07 ± 2.19%	17.56 ± 1.37%
Periaqueductal gray	21.79 ± 0.92%	21.15 ± 2.58%
Dorsal raphe nuclei	24.25 ± 1.44%	21.29 ± 2.28%
Locus coeruleus	35.83 ± 2.03%	32.93 ± 0.60%
Cortical area	**Ipsilateral**	**Contralateral**
Area Cg1—Layer V	60.21 ± 2.25%	49.40 ± 3.43%
Area PrL—Layer V	51.11 ± 2.87%	43.56 ± 2.01%
Area PrL—Layer VI	37.25 ± 2.48%	36.03 ± 1.36%
Area IL—Layer V	52.28 ± 2.96%	40.69 ± 2.71%
Area IL—Layer VI	33.96 ± 3.00%	36.30 ± 1.05%

The cell counts shown are derived from analyses of every brain area where appreciable retrograde labeling was found (more than 50 cells per region per subject) and were made on per animal (n = 5), per area, and per hemisphere (ipsilateral and contralateral to the injection site) bases. For every cortical and subcortical site reported, values are based on evaluation of 50–600 back-labeled cells per site, per side, per animal subject.

assessment of extracellular PFC DA levels in sham-operated CTRL, GDX, GDX-E, and GDX-TP rats. The effectiveness of the hormone treatments in all subjects was confirmed by the weights of their androgen-sensitive BSMs. As expected, the mean muscle weights of the CTRL and GDX-TP rats for both the APV and the NBQX studies were similar to each other and some 4-fold higher than those of the GDX and GDX-E rat groups (Table 2). ANOVAs identified significant main effects of hormone treatment on BSM weight (APV group: $F_{3,18}$ = 339.654, P < 0.0001; NBQX group: $F_{3,18}$ = 287.414, P < 0.0001) and post hoc comparisons confirmed that for both groups the BSM weights of the CTRL and GDX-TP groups were similar and not significantly different from one another, the weights of the GDX and GDX-E rats were similar and not significantly different from each other, and the BSM weights of the GDX and GDX-E groups were significantly different from those of both the CTRL and the GDX-TP groups. The effectiveness of hormone treatments was also reflected in group differences in resting extracellular PFC DA levels. As expected (Aubele and Kritzer 2011), basal extracellular PFC DA levels in the CTRL and GDX-TP cohorts were similar to each and were roughly half that measured in the GDX and GDX-E rat groups for both the NBQX and the APV studies (Table 2). ANOVAs identified significant main effects of hormone treatment on resting PFC DA level (APV group: $F_{3,18}$ = 9.815, P = 0.0008; NBQX group $F_{3,18}$ = 10.822, P = 0.0006), and post hoc comparisons confirmed that predrug basal DA concentration in GDX and GDX-E but not GDX-TP rats was significantly higher than CTRL animals (P < 0.0001).

AMPA Receptor Antagonism

Within 40–60 min of infusion of the selective AMPA antagonist NBQX, PFC DA levels in CTRL rats of this study decreased by

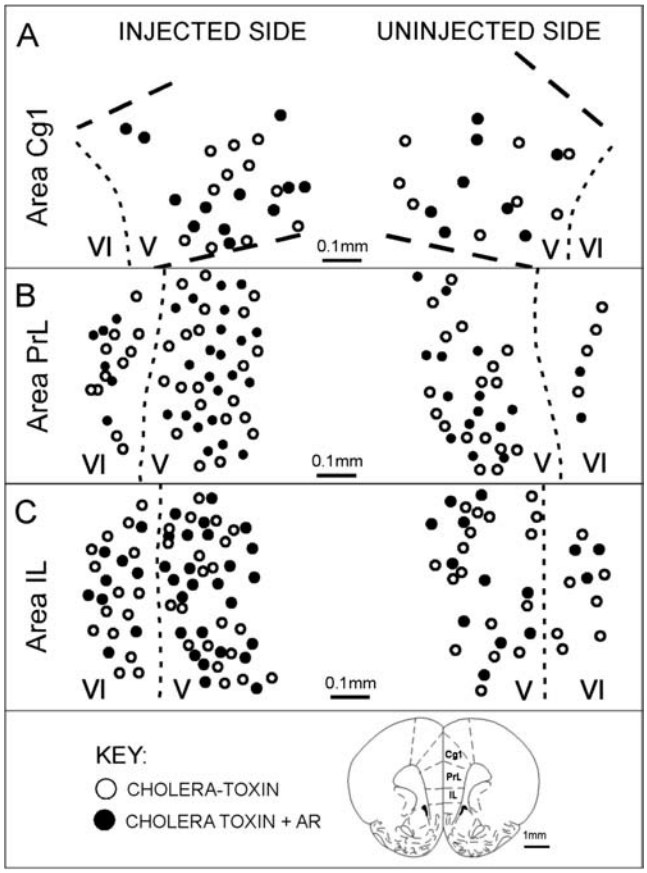

Figure 5. (*A*) Representative camera lucida drawings replotted onto section outlines adapted from Paxinos and Watson (1998), showing the location of medial prefrontal cortical neurons that were retrogradely labeled by cholera toxin injection in the VTA (open circles) and of neurons that were both retrogradely labeled and immunoreactive for AR (black circles). Labeling within areas Cg1, PrL, and IL from hemispheres ipsilateral (injected, left-hand side) and contralateral (uninjected, right-hand side) to the injection site is shown; laminar boundaries are marked by dashed lines and layers are identified by Roman numerals. Back-labeled cells were all confined to layers V and VI. From one-third to more than half of these cells were immunoreactive for AR.

Table 2
Mean BSM weights (g) and resting extracellular PFC DA levels (fmol/uL) ± standard error of the mean for groups of rats that were sham-operated (CTRL), gonadectomized (GDX), or gonadectomized and supplemented with testosterone propionate (GDX-TP) or with estradiol (GDX-E)

AMPA antagonist study	BSM weight (g)	Resting DA level (fmol/μL)
CTRL (n = 5)	1.26 ± 0.04	0.153 ± 0.003
GDX (n = 5)	0.39 ± 0.02**	0.289 ± 0.010**
GDX-TP (n = 5)	1.29 ± 0.04	0.146 ± 0.004
GDX-E (n = 4)	0.33 ± 0.02**	0.317 ± 0.003**
NMDA antagonist study	BSM weight (g)	Resting DA level (fmol/μL)
CTRL (n = 5)	1.25 ± 0.04	0.136 ± 0.002
GDX (n = 5)	0.36 ± 0.02**	0.267 ± 0.014**
GDX-TP (n = 5)	1.28 ± 0.03	0.132 ± 0.008
GDX-E (n = 4)	0.33 ± 0.02**	0.254 ± 0.009**

Data from the cohorts of animals that were used for microdialysis/reverse dialysis experiments utilizing glutamate AMPA and NMDA receptor antagonists are shown separately. As expected, the efficacy of hormone treatments in both sets of animal subjects was reflected in mean BSM weights that were significantly lower and resting extracellular DA levels that were significantly higher in GDX and GDX-E compared with the CTRL and GDX-TP groups (ANOVA, followed by Fisher's PLSD post hoc comparison, $^{**}P < 0.05$).

approximately 30–40% and remained at these depressed levels for the duration of the drug application period (Fig. 6*A*). After drug offset, DA levels returned to stable predrug levels within about 80 min (Fig. 6*A*). Quantitatively and qualitatively similar effects of NBQX infusion were also seen in the GDX-TP group (Fig. 6*A*). However, in the GDX and GDX-E rats, infusion of NBQX had no discernable effect on PFC DA level. Rather, for both groups, PFC DA levels remained within 10% of predrug baseline values for the entire drug application and postapplication period (Fig. 6*A*). A stepwise series of statistical analyses supported the robustness of these group differences in drug response. First, a 2-way mixed-model ANOVA with a repeated measures design identified significant main effects of group ($F_{3,38}$ = 6.589, P <0.001) as well as a significant interaction between group and time ($F_{3,38}$ = 7.320, P < 0.001). These analyses were followed by within-group 1-way ANOVAs with repeated measures designs using DA levels from each 20-min sample as within-subjects factor that identified significant main effects of time on PFC DA levels in the CTRL and GDX-TP ($F_{2.782,32.5}$ = 4.605–4.971, P = 0.048–0.031) but not the GDX or GDX-E groups ($F_{2.782,32.5}$ = 0.489–1.047, P = 0.48–0.27). Allowed post hoc comparisons of these data further showed that for all of the hormone treatment groups, none of the predrug and postdrug DA samples differed from one another, that baseline DA samples were significantly higher than those measured from 80 min after drug onset until its offset in the CTRL and GDX-TP cohorts (P= 0.031–0.047), and that in the GDX and GDX-E rats DA samples obtained before, during, or after drug application did not differ from one another. Finally, 1-way ANOVAs that compared DA level for corresponding 20-min sample periods between groups revealed significant main effects of hormone treatment on drug-induced changes in PFC DA level for time points ranging from 80 min after drug onset until its offset ($F_{3,38}$ = 3.831–6.589, P= 0.041–0.01). The allowed post hoc comparisons that followed further showed that drug-depressed DA levels in the CTRL and GDX-TP groups were similar to each other, that drug-insensitive DA levels in the GDX and GDX-E groups were similar to each other, and that local AMPA antagonism yielded DA levels in the PFC of CTRL and GDX-TP rats that were significantly different from those in the GDX and GDX-E groups during the identified time periods (all P < 0.05, see Fig. 6*A*).

NMDA Receptor Antagonism

Within 20 min of onset, reverse dialysis infusion of the selective NMDA antagonist APV into the mPFC increased extracellular PFC DA levels in CTRL animals by about 20% (Fig. 6*B*). Within 60 min DA levels increased further and plateaued at concentrations that were about 40% higher than predrug baseline; DA concentrations remained at these levels for the duration of the drug application period. Following drug offset, DA levels returned to stable predrug levels within 40–60 min (Fig. 6*B*). Similar effects of drug infusion were observed in GDX-TP rats, albeit with DA levels rising about 15% higher, and taking roughly 60 min longer to return to predrug levels after drug offset (Fig. 6*B*). In contrast, APV infusion in the GDX and GDX-E rats "decreased" PFC DA levels (Fig. 6*B*). Within 20 min of drug onset, DA levels in both groups dropped by about 20% and fell further over the next 20 min to reach maximally depressed levels that were roughly 40% lower than baseline that remained for the duration of the drug application period (Fig. 6*B*). Following drug offset, DA levels in these 2 groups returned to predrug values by 60–80 min (Fig. 6*B*).

Statistical assessments confirmed the significance of these group differences in drug response. Specifically, a 2-way mixed-model ANOVA with a repeated measures design first identified

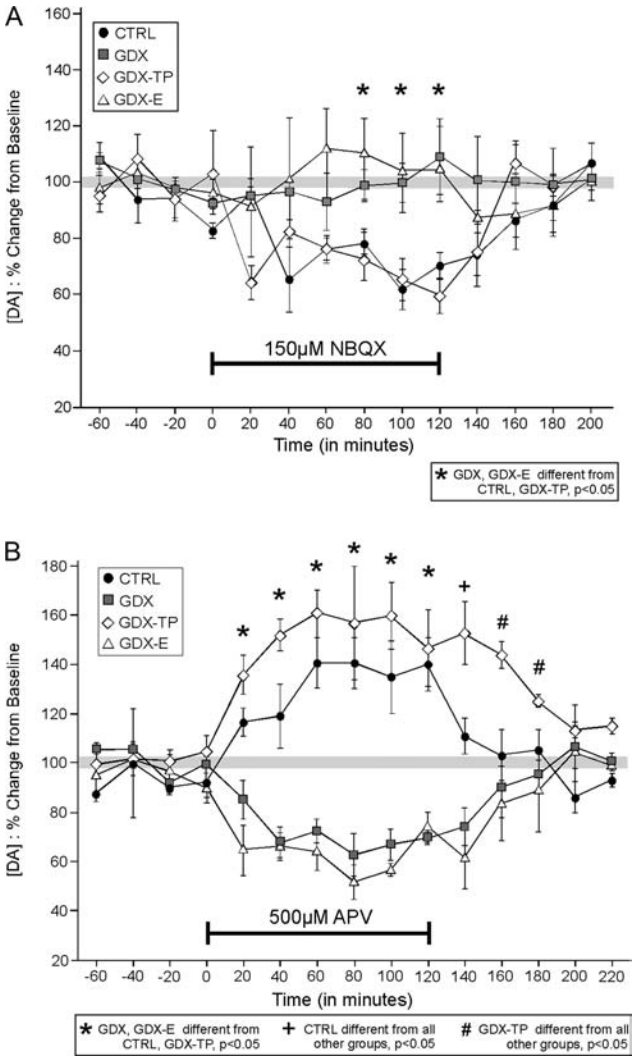

Figure 6. (*A*) Timelines showing the effect of reverse dialysis application of NBQX (*A*) and of APV (*B*) on PFC extracellular DA levels expressed as mean percent change from baseline (±standard error of the mean) in control (CTRL, black circles), gonadectomized (GDX, gray squares), and GDX rats supplemented with testosterone propionate (GDX-TP, white diamonds) or with estradiol (GDX-E, white triangles). Within 20 min of application, NBQX decreased extracellular DA levels in CTRL and GDX-TP rats B but had no measureable effect on DA levels in the GDX or GDX-E groups (*A*). The reverse dialysis application of APV on the other hand increased prefrontal DA levels in the CTRL and GDX-TP groups but decreased DA levels in GDX and GDX-E rats. Asterisks identify all time points during the studies when drug effects on DA levels in GDX and GDX-E animals are significantly different than that in CTRL and GDX-TP groups. A plus sign (+) indicates the time point when DA levels in CTRL rats were significantly different from all other groups and pound signs (#) indicate times when DA levels in GDX-TP rats were significantly different from all other groups.

a significant main effect of group ($F_{3,38}$ = 21.918, P < 0.001) and a significant interaction between group and time ($F_{3,38}$ = 33.231, P < 0.001). This was followed by a series of within-group 1-way ANOVAs with repeated measures designs that used DA levels from each 20-min time sample as within-subjects factor. These analyses identified significant to near-significant main effects of time on PFC DA level for all hormone treatment groups ($F_{2.912,32.5}$ = 3.739–6.566, P = 0.0809–0.009) and allowed post hoc comparisons further confirmed that for all groups, predrug and postdrug baseline DA samples were similar to each other and were significantly different (P < 0.05) from DA levels measured from 20 min after drug application until its cessation. Post hoc comparisons also supported the robustness of observed group differences in the time it took DA levels to return to baseline after drug offset. Specifically, 20 min after drug offset DA levels in the GDX, GDX-E, and GDX-TP rats were significantly different from CTRL, and over the next 40 min DA levels in the GDX-TP cohort were significantly different from that of all other groups (all P < 0.05, see Fig. 6*B*). Lastly, a series of 1-way ANOVAs run for each 20-min time period across animal groups revealed main effects of hormone treatment on drug-induced changes in PFC DA level that were significant from 20 min after drug onset to 60 min after drug offset ($F_{3,38}$ = 21.345–22.847, P = 0.0001–0.0005). Post hoc comparisons of these data also showed that the effects of APV on PFC DA levels were similar in CTRL and GDX-TP rats, and were similar in GDX and GDX-E rats, but were significantly different in the CTRL and GDX-TP compared with GDX and GDX-E cohorts from 20 min after drug onset until 60 min after drug offset (all P < 0.05, Fig. 6*B*).

Discussion

Findings including parallel androgen-sensitive effects of GDX in adult male rats on DA-dependent behaviors, DA axon density, and resting extracellular DA levels are just some of the evidence linking hormone influence over PFC function in males to androgen modulation of PFC DA systems (Kritzer 2000, 2003; Kritzer et al. 2001, 2007; Aubele et al. 2008; Aubele and Kritzer 2011). Correlations between high circulating testosterone levels and DA-dependent PFC functions in healthy human males and between low testosterone titers and PFC dysfunction in male patient populations including diagnosed schizophrenics (Cherrier et al. 2007; Ko et al. 2007; Nelson et al. 2007; Young et al. 2010) further emphasize the need to better understand the mechanisms of androgen action that may be involved. As a first step, the studies presented here combined tract tracing and immunocytochemistry to determine where, among circuits associated with the PFC DA system, the intracellular receptors necessary for genomic androgen actions are located. These analyses revealed that projections from the PFC to the VTA were the most AR enriched of all pathways projecting either to or from mesoprefrontal DA cells of origin. This aligns a predictably potent genomic androgen influence with glutamatergic corticofugal projections well known to regulate ventral midbrain cell firing (Gonon 1988; Gariano et al. 1989; Overton and Clark 1997; Schultz 1998) and in turn extracellular PFC DA levels (Jedema and Moghddam 1996; Takahata and Moghaddam 1998; Westerink et al. 1998; Moghaddam 2003). The previously unsuspected possibility that androgens modulate glutamate's influence over PFC DA was explored in second set of studies that utilized an established in vivo microdialysis/drug challenge protocol and AMPA and NMDA subtype-selective antagonists to compare the expected effects of these drugs on PFC DA levels in CTRL, GDX, GDX-E, and GDX-TP rats. These revealed that GDX induced an androgen-sensitive, estrogen-insensitive decrease in PFC DA response to AMPA antagonism and a highly aberrant depressive response to NMDA antagonism. This indicates that under normal conditions androgen exerts a dual influence that simultaneously promotes AMPA-mediated stimulation and inhibits NMDA-mediated stimulation of an excitatory influence(s) that tonically regulates mesoprefrontal DA systems. As discussed below, microdialysis data are considered

along with a) known details of PFC circuit structure, b) the known actions of local PFC AMPA and NMDA antagonism on its DA levels, and c) the AR enrichment in PFC-to-VTA–projecting pyramidal cells identified here to develop a working model that includes central roles for these corticofugal afferents in androgen's regulation and GDX's dysregulation of PFC DA tone. The limited number of previous studies examining hormone effects on glutamate receptors in other areas of the male brain that support this scenario are also discussed.

Novel Substrates for Genomic Androgen Regulation of Prefrontal DA Systems

A considerable literature describes sex differences and/or gonadal hormone sensitivity of PFC DA systems and the complex cognitive functions they support in both humans and animal models. Furthermore, there is consensus for androgens in particular being the primary hormone modulators of these systems and functions in males. To begin to understand how this androgen influence might be conferred, previous studies in adult male rats asked whether underlying genomic hormone actions were likely to directly engage mesoprefrontally projecting DA cells of the VTA. This was accomplished by determining whether and to what extent intracellular ARs were present within VTA neurons that were dually identified as DAergic and as projecting to the PFC (Kritzer and Creutz 2008). Previous studies had demonstrated colocalization of immunoreactivity for AR and for the DA marker tyrosine hydroxylase within a substantial number of cells in the paranigral and parabrachial portions of the VTA (Kritzer 1997). Surprisingly, however, when additionally identified by their connections, relatively few of these AR-IR, DAergic cells were found to project to the PFC (Kritzer and Creutz 2008). That in males only some 20–25% of prefrontally projecting DA neurons contained AR (Kritzer and Creutz 2008) suggests that VTA DA neurons themselves may not be the primary place where genomic androgen influence over PFC DA systems is brought to bear. Here, combined immunocytochemical and tract-tracing studies strategies took the question of anatomical substrates one synapse back and asked whether projections that are afferent to the VTA might instead be a more robust route for androgen influence. For all but 2 of more than 20 subcortical projections to the VTA assessed, however, no to very low proportions of these cells of origin were found to contain AR immunoreactivity. Furthermore, while inputs arising from the locus coeruleus and raphe nuclei had the highest incidence of AR colocalization, even these subcortical zones had only some 20–35% of VTA-projecting neurons that were AR-IR. Thus, the degree to which genomic androgen influence over PFC DA systems is conferred via subcortical afferents to the VTA is likely less than or at best equal to the modest influence expected to be exerted directly upon mesoprefrontal DA cells themselves.

In addition to subcortical inputs, however, the VTA also receives a substantial innervation from the infragranular layers of the mPFC (Au-Young et al. 1999; Carr and Sesack 2000; Sesack and Carr 2002). Our analyses of labeling in these cortical fields revealed proportions of AR-IR projection neurons that were much higher than for any other pathway associated with the PFC DA system examined to date. Specifically, in all retrogradely labeled PFC fields, AR-containing afferents made up close to—and in some cases more than half of the PFC-to-VTA projection pathway.

Previous studies have shown that AR is present in large numbers of pyramidal cells in both the supragranular and the infragranular layers of many areas of the cerebral cortex including the PFC (Clark et al. 1988; Finley and Kritzer 1999; Nunez et al. 2003; Kritzer 2004). In rats, a majority of the AR-IR pyramids present in the supragranular layers of the PFC have been further identified as those engaged in making associational and contralateral corticocortical connections (Kritzer 2004). However, a survey of corticocortical, corticothalamic, corticostriatal, corticoaccumbal, and corticocollicular connections found that very few of the AR-IR pyramidal cells present in the PFC's infragranular layers participated in any of these projections (Kritzer 2004). That significant proportions of these cells were found in this study to take part in corticofugal projections to the VTA thus gives a connectional signature to this substantial yet heretofore incompletely defined cell group. These findings also align AR-IR with a pathway that is well known to regulate PFC DA levels, in part via the monosynaptic contacts it makes onto midbrain DA neurons that in return project directly back to the PFC (Carr et al. 1999; Carr and Sesack 2000). In the section that follows, data from the present microdialysis/reverse dialysis drug application studies that provide evidence for androgen sensitivity of these key corticofugal projections are synthesized with these anatomical findings to formulate a novel working model for androgen stimulation of DA systems in the male PFC.

A Working Model for Genomic Androgen Modulation of PFC DA Systems

The AR-IR, VTA-projecting PFC pyramidal cells identified in this study are part of a descending pathway that tonically regulates single spiking ventral midbrain activity, that phasically stimulates midbrain bursting activity and that regulates the feedforward metric of DA level within the PFC (Gariano and Groves 1988; Gonon 1988; Overton et al. 1996; Tong et al. 1996b; Overton and Clark 1997). Previous studies have shown that in addition to local presynaptic PFC actions (Schoepp et al. 1995), reverse dialysis application of selective AMPA receptor agonists and/or antagonists in the PFC can also drive and inhibit these PFC-to-VTA afferent projections, respectively, and in turn increase and decrease extracellular PFC DA levels (Jedema and Moghddam 1996; Takahata and Moghaddam 1998). Administration of NMDA receptor agonists and/or antagonists, on the other hand, has been shown to both directly and presumably presynaptically influence PFC DA release (Grilli et al. 2009) and indirectly act on the PFC's fast spiking, presumed parvalbumin (PV)-positive -aminobutyric acid (GABA)ergic interneurons to inhibit and disinhibit VTA-projecting pyramids and lower and raise extracellular PFC DA levels, respectively (Verma and Moghaddam 1996; Takahata and Moghaddam 1998; Moghaddam 2003; Sesack et al. 2003; Homayoun and Moghaddam 2007; Pratt et al. 2008). When local antagonist application strategies were used here to assess the patency of glutamatergic PFC DA-regulating systems under conditions of long-term hormone deprivation and/or replacement, evidence was found for a GDX-induced androgen-sensitive diminution in the tonic AMPA-mediated drive that normally elevates PFC DA levels, and a qualitative shift in what are normally inhibitory NMDA-mediated influences to ones that tonically increase PFC DA levels in adult male rats. The working model that we propose to explain these findings involves GDX-induced changes in the

glutamate receptivity of the AR-bearing, VTA-projecting PFC pyramidal cells identified in the first part of this study and the excitability of their intracortical and/or corticofugal connections (see Fig. 7).

There are several arguments that support the possibility that the anomalous responses to glutamate stimulation observed in this study may be due to changes in AMPA and NMDA receptivity/signaling within AR-bearing, VTA-projecting PFC pyramidal cells. Foremost, this interpretation localizes causative effects to cells containing the receptive machinery necessary for the genomic androgen actions that are presumed to be at work. It also explains outcomes in terms of mechanisms that bypass PFC PV interneurons which are neither expected to be involved based on their AR immunonegativity (Kritzer 2006) nor easily reconciled with the findings obtained here with respect to APV. It is further possible and perhaps even likely that hormone influence over glutamate signaling as mediated by these cells extends to both their intracortical and their corticofugal connections. Accordingly, the working model also accounts for hormone actions as potentially affecting both the presynaptic intracortical glutamatergic mechanisms (Schoepp et al. 1995; Rodvelt et al. 2008; Grilli et al. 2009; Livingstone et al. 2010) and/or the postsynaptic tegmental glutamatergic mechanisms that have been shown to be active in the regulation of PFC DA homeostasis and tone.

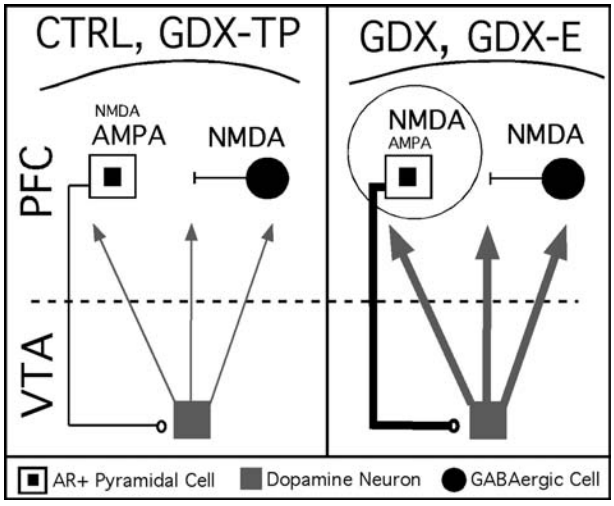

Figure 7. Circuit diagram of a working model for androgen influence over mesoprefrontal DA levels. This study showed that pyramidal cells projecting from PFC to the VTA contain intracellular ARs (white squares with black centers). The output of these pyramids is well known to provide a tonic excitatory drive onto mesoprefrontally projecting DA neurons (gray square) that is normally a balance of direct AMPA-mediated excitation and disynaptic inhibition resulting from NMDA-mediated excitation of local GABAergic interneurons (black circle). In this working model, androgen is critical in maintaining the AMPA sensitivity and a relative NMDA insensitivity of these AR-bearing corticofugal pyramids. Thus, in control animals (CTRL) and in gondadectomized rats supplemented with testosterone (GDX-TP) where androgen influence is preserved, AMPA antagonism decreases and NMDA antagonism increases activity in these pyramidal cells, in midbrain DA cells and ultimately in PFC DA levels, and normal resting PFC DA levels are observed (left panel). However, in gonadectomized rats (GDX) and in gonadectomized rats given estradiol (GDX-E, right panel) where androgen influence is diminished, there results an aberrant increase in sensitivity to NMDA-mediated stimulation and a decrease in the sensitivity to AMPA-mediated stimulation within this pathway. This is consistent with the reduced effect of AMPA antagonism and can also explain the highly abnormal decreases in PFC DA level that NMDA antagonism produces in GDX and GDX-E animals. The hyperexcitability that an increase in the ratio of NMDA-to-AMPA transmission is also likely to yield (thicker pyramidal cell axon, right panel) would also result in increased basal stimulation of the VTA and thus account for the increased DA overflow at rest (thicker DA cell axons) that is also observed in GDX and GDX-E rats.

Although there have been relatively few investigations of hormone effects on AMPA and NMDA signaling in males, there is also some precedent for GDX in adult male rats to decrease measures of AMPA receptors, to increase NMDA receptor binding and receptor-mediated actions, and to do so specifically within AR-enriched regions of the brain. In the hypothalamus, for example, some 45–55% of neurons colocalize immunoreactivity for GluR1 or GluR2/3 AMPA receptor subunits and AR, and long-term GDX has been shown to significantly decrease and testosterone replacement increase GluR1 and GluR2/3 protein levels (Diano et al. 1997). In contrast, in septal and amygdaloid nuclei where most GluR1 and 2/3 immunopositive cells are AR immunonegative, GDX and hormone replacement are without effect on AMPA receptor subunit proteins (Diano et al. 1997). In hippocampus and/or retrosplenial cortex, on the other hand, long-term GDX has been shown to increase ^{125}I MK801 binding, elevate physiological measures of NMDA-dependent plasticity including LTP and to potentiate neurotoxic effects of NMDA relative to GDX rats treated with TP, dihydrotestosterone, or dihydrotestosterone propionate (Kus et al. 1995; Harley et al. 2000).

It may also be important to note that genomic effects of estradiol treatment in ovariectomized female rats have been shown to induce changes in the ratios of NMDA/AMPA transmission in hippocampal pyramidal cells (Smith and McMahon 2005) in much the same way as is postulated here for PFC pyramids in males. Specifically, while effects of estradiol and the estrus cycle to potentiate numerous measures of hippocampal and PFC pyramidal cell excitability are well known (McEwen 1996; Woolley 1998; McEwen 2002; Smith et al. 2009), it has been recently shown that some of these excitatory effects are dependent on and time locked to induced increases in the ratio of NMDA-to-AMPA cell signaling (Smith and McMahon 2005). Applying a similar scenario to the postulated increase in NMDA-to-AMPA receptivity/transmission in AR-IR, VTA-projecting pyramidal cells in the male PFC thus predicts an increased excitability of this corticofugal pathway in GDX and GDX-E but not CTRL or GDX-TP rats. Given the wealth of electrophysiological data showing that increased activity within this descending projection increases mesoprefrontal DA cell firing and extracellular PFC DA levels (Gariano and Groves 1988; Gonon 1988; Svensson and Tung 1989; Overton et al. 1996; Tong et al. 1996a, 1996b; Overton and Clark 1997; Gao et al. 2007; Lodge 2011), the working model proposed not only fits the data from drug-stimulation studies but could also explain the higher than normal extracellular PFC DA levels that characterize GDX and GDX-E but not CTRL or GDX-TP rats at rest (Aubele and Kritzer 2011). The model also provides for the possibility of an increase in the excitatory drive of the intracortical connections of these cells, which based on evidence from PFC slices and synaptosomal preparations for local, presumed presynaptic NMDA (Rodvelt et al. 2008; Grilli et al. 2009; Livingstone et al. 2010) and AMPA-mediated (Schoepp et al. 1995; Livingstone et al. 2010) stimulation of PFC DA release would also be consistent with findings in the hormone treatment groups under basal and drug-stimulated conditions.

Formulated primarily on the premise that loci for the long-term androgen actions at work are AR-bearing, it is important to keep in mind that the working model that is hypothesized does not preclude involvement of additional androgen-sensitive

substrates, including the modest populations of DAergic VTA-to-PFC projection neurons that have been previously identified as AR-IR (Lu et al. 2000; Kritzer and Creutz 2008). Indeed, parallel changes in NMDA-to-AMPA receptivity/signaling taking place within the glutamatergic PFC-to-VTA–projecting neurons and/or within the cells making up the returning DAergic VTA-to-PFC pathways could provide a synergy of effects that may be necessary for the large, typically severalfold group differences in basal and drug-stimulated PFC DA levels that are induced by GDX. It is also currently unresolved whether and to what extent the abnormalities observed in glutamate-stimulated PFC DA reflect intracortical versus tegmental processes. While cell-specific electrophysiological approaches will ultimately be required to establish the validity and elucidate essential details of the working model proposed here, it may also be instructive for future studies to explore the effects of GDX and hormone replacement on elevations in PFC DA level under varying behavioral contexts. For example, recent evidence showing that hypotension-induced elevations in PFC DA level are mediated by intracortical but not tegmental glutamatergic signaling (Kawahara et al. 2002) could help clarify whether and to what extent GDX influences are translated through local versus afferent glutamatergic circuits. Finally, additional directions for research might also explore intracellular signaling cascades, kinases, and phosphorylases as potential mediators of the complex effects that are observed. Given the opposing actions of androgen on NMDA versus AMPA signaling that the model invokes, protein kinase C stands out as a moiety of particular interest as it is an identified target of AR-dependent androgen signaling in neurons (Nguyen et al. 2009) whose phosphorylation of NMDA receptors has been shown to increase calcium-dependent receptor inactivation (Lu et al. 2000) and whose phosphorylation of specific threonine residues of AMPA receptors has been shown to increase their cell surface expression and facilitate excitatory transmission (Lee et al. 2007, 2010).

Summary and Conclusions

Converging anatomical, physiological, and behavioral data provide strong support for selective and important roles for androgen stimulation in maintaining PFC DA systems and DA-dependent PFC processes in males. The data presented here now suggest that glutamate signaling should be brought into the equation of hormone and specifically androgen modulation of PFC DA systems and DA-dependent functions in this sex. Impetus to pursue the means and mechanisms underlying this novel avenue for hormone action in males comes from the contemporary glutamate hypotheses for PFC function and perhaps even more so for its dysfunction in disorders such as schizophrenia, autism, and attention deficit hyperactivity disorder (Moghaddam 2003; Lewis and Moghaddam 2006; Javitt 2007; Arnsten 2009; Scott and Aperia 2009; Seeman 2009; Javitt 2010; Marek et al. 2010). For all of the advances that have been made in treating these disorders, their prefrontal symptoms remain notoriously recalcitrant to therapeutic intervention and extremely disabling. That these symptoms also more often and more severely affect males (Rucklidge 2008; Zahn-Waxler et al. 2008; Ramtekkar et al. 2010), that their severity has been repeatedly correlated with testosterone level (Patwardhan et al. 2000; Cherrier et al. 2001; Shirayama et al. 2002; Strous et al. 2003; Goyal et al. 2004; Taherianfard and Shariaty 2004; Akhondzadeh et al. 2006; Janowsky 2006; Cherrier et al. 2007; Geier and Geier 2007; Ko et al. 2007; Nelson et al. 2007), and that they have recently been shown to be ameliorated by testosterone augmentation as an adjunct to conventional drug therapies in schizophrenia (Strous et al. 2003; Ko et al. 2008) gives urgency to issues of resolving androgen's roles in modulating the DA-dependent PFC systems and processes that are at risk in these disorders.

Funding

National Institutes of Neurological Disorder and Stroke (RO1-NS41966 to M.F.K.).

Notes

The outstanding technical support of Ms Aiying Liu and Ms Jessica Giacinto is gratefully acknowledged. *Conflict of Interest*: None declared.

References

Adler A, Vescovo P, Robinson JK, Kritzer MF. 1999. Gonadectomy in adult life increases tyrosine hydroxylase immunoreactivity in the prefrontal cortex and decreases open field activity in male rats. Neuroscience. 89:939–954.

Akhondzadeh S, Rezaei F, Larijani B, Nejatisafa AA, Kashani L, Abbasi SH. 2006. Correlation between testosterone, gonadotropins and prolactin and severity of negative symptoms in male patients with chronic schizophrenia. Schizophr Res. 84:405–410.

Arnsten AF. 2009. Toward a new understanding of attention-deficit hyperactivity disorder pathophysiology: an important role for prefrontal cortex dysfunction. CNS Drugs. 23(Suppl 1):33–41.

Aubele T, Kaufman R, Montalmant F, Kritzer MF. 2008. Effects of gonadectomy and hormone replacement on a spontaneous novel object recognition task in adult male rats. Horm Behav. 54:244–252.

Aubele T, Kritzer MF. 2011. Gonadectomy and hormone replacement affects in vivo Basal extracellular dopamine levels in the prefrontal cortex but not motor cortex of adult male rats. Cereb Cortex. 21:222–232.

Au-Young SM, Shen H, Yang CR. 1999. Medial prefrontal cortical output neurons to the ventral tegmental area (VTA) and their responses to burst-patterned stimulation of the VTA: neuroanatomical and in vivo electrophysiological analyses. Synapse. 34:245–255.

Carr DB, O'Donnell P, Card JP, Sesack SR. 1999. Dopamine terminals in the rat prefrontal cortex synapse on pyramidal cells that project to the nucleus accumbens. J Neurosci. 19:11049–11060.

Carr DB, Sesack SR. 2000. Projections from the rat prefrontal cortex to the ventral tegmental area: target specificity in the synaptic associations with mesoaccumbens and mesocortical neurons. J Neurosci. 20:3864–3873.

Ceccarelli I, Scaramuzzino A, Aloisi AM. 2001. Effects of gonadal hormones and persistent pain on non-spatial working memory in male and female rats. Behav Brain Res. 123:65–76.

Cherrier MM, Asthana S, Plymate S, Baker L, Matsumoto AM, Peskind E, Raskind MA, Brodkin K, Bremner W, Petrova A, et al. 2001. Testosterone supplementation improves spatial and verbal memory in healthy older men. Neurology. 57:80–88.

Cherrier MM, Matsumoto AM, Amory JK, Johnson M, Craft S, Peskind ER, Raskind MA. 2007. Characterization of verbal and spatial memory changes from moderate to supraphysiological increases in serum testosterone in healthy older men. Psychoneuroendocrinology. 32:72–79.

Clark AS, MacLusky NJ, Goldman-Rakic PS. 1988. Androgen binding and metabolism in the cerebral cortex of the developing rhesus monkey. Endocrinology. 123:932–940.

Collins WF, 3rd, Seymour AW, Klugewicz SW. 1992. Differential effect of castration on the somal size of pudendal motoneurons in the adult male rat. Brain Res. 577:326–330.

Dalley JW, Cardinal RN, Robbins TW. 2004. Prefrontal executive and cognitive functions in rodents: neural and neurochemical substrates. Neurosci Biobehav Rev. 28:771–784.
Daniel JA, Abrams MS, deSouza L, Wagner CG, Whitlock BK, Sartin JL. 2003. Endotoxin inhibition of luteinizing hormone in sheep. Domest Anim Endocrinol. 25:13–19.
Diano S, Naftolin F, Horvath TL. 1997. Gonadal steroids target AMPA glutamate receptor-containing neurons in the rat hypothalamus, septum and amygdala: a morphological and biochemical study. Endocrinology. 138:778–789.
DonCarlos LL, Sarkey S, Lorenz B, Azcoitia I, Garcia-Ovejero D, Huppenbauer C, Garcia-Segura LM. 2006. Novel cellular phenotypes and subcellular sites for androgen action in the forebrain. Neuroscience. 138:801–807.
Egan MF, Goldberg TE, Kolachana BS, Callicott JH, Mazzanti CM, Straub RE, Goldman D, Weinberger DR. 2001. Effect of COMT Val108/158 Met genotype on frontal lobe function and risk for schizophrenia. Proc Natl Acad Sci U S A. 98:6917–6922.
Feenstra MG, Botterblom MH, van Uum JF. 2002. Behavioral arousal and increased dopamine efflux after blockade of NMDA-receptors in the prefrontal cortex are dependent on activation of glutamatergic neurotransmission. Neuropharmacology. 42:752–763.
Feenstra MG, van der Weij W, Botterblom MH. 1995. Concentration-dependent dual action of locally applied N-methyl-D-aspartate on extracellular dopamine in the rat prefrontal cortex in vivo. Neurosci Lett. 201:175–178.
Feng Y, Weijdegard B, Wang T, Egecioglu E, Fernandez-Rodriguez J, Huhtaniemi I, Stener-Victorin E, Billig H, Shao R. 2010. Spatiotemporal expression of androgen receptors in the female rat brain during the oestrous cycle and the impact of exogenous androgen administration: a comparison with gonadally intact males. Mol Cell Endocrinol. 321:161–174.
Finley SK, Kritzer MF. 1999. Immunoreactivity for intracellular androgen receptors in identified subpopulations of neurons, astrocytes and oligodendrocytes in primate prefrontal cortex. J Neurobiol. 40:446–457.
Gao M, Liu CL, Yang S, Jin GZ, Bunney BS, Shi WX. 2007. Functional coupling between the prefrontal cortex and dopamine neurons in the ventral tegmental area. J Neurosci. 27:5414–5421.
Gariano RF, Groves PM. 1988. Burst firing induced in midbrain dopamine neurons by stimulation of the medial prefrontal and anterior cingulate cortices. Brain Res. 462:194–198.
Gariano RF, Sawyer SF, Tepper JM, Young SJ, Groves PM. 1989. Mesocortical dopaminergic neurons. 2. Electrophysiological consequences of terminal autoreceptor activation. Brain Res Bull. 22:517–523.
Geier DA, Geier MR. 2007. A prospective assessment of androgen levels in patients with autistic spectrum disorders: biochemical underpinnings and suggested therapies. Neuro Endocrinol Lett. 28:565–573.
Geisler S, Zahm DS. 2005. Afferents of the ventral tegmental area in the rat-anatomical substratum for integrative functions. J Comp Neurol. 490:270–294.
Gibbs RB, Johnson DA. 2008. Sex-specific effects of gonadectomy and hormone treatment on acquisition of a 12-arm radial maze task by Sprague Dawley rats. Endocrinology. 149:3176–3183.
Goldberg TE, Egan MF, Gscheidle T, Coppola R, Weickert T, Kolachana BS, Goldman D, Weinberger DR. 2003. Executive subprocesses in working memory: relationship to catechol-O-methyltransferase Val158Met genotype and schizophrenia. Arch Gen Psychiatry. 60:889–896.
Goldman-Rakic PS, Funahashi S, Bruce CJ. 1990. Neocortical memory circuits. Cold Spring Harb Symp Quant Biol. 55:1025–1038.
Gonon FG. 1988. Nonlinear relationship between impulse flow and dopamine released by rat midbrain dopaminergic neurons as studied by in vivo electrochemistry. Neuroscience. 24:19–28.
Goyal RO, Sagar R, Ammini AC, Khurana ML, Alias AG. 2004. Negative correlation between negative symptoms of schizophrenia and testosterone levels. Ann N Y Acad Sci. 1032:291–294.
Grilli M, Pittaluga A, Merlo-Pich E, Marchi M. 2009. NMDA-mediated modulation of dopamine release is modified in rat prefrontal cortex and nucleus accumbens after chronic nicotine treatment. J Neurochem. 108:408–416.
Hamson DK, Jones BA, Watson NV. 2004. Distribution of androgen receptor immunoreactivity in the brainstem of male rats. Neuroscience. 127:797–803.
Harley CW, Malsbury CW, Squires A, Brown RA. 2000. Testosterone decreases CA1 plasticity in vivo in gonadectomized male rats. Hippocampus. 10:693–697.
Homayoun H, Moghaddam B. 2007. NMDA receptor hypofunction produces opposite effects on prefrontal cortex interneurons and pyramidal neurons. J Neurosci. 27:11496–11500.
Janowsky JS. 2006. The role of androgens in cognition and brain aging in men. Neuroscience. 138:1015–1020.
Janowsky JS, Chavez B, Orwoll E. 2000. Sex steroids modify working memory. J Cogn Neurosci. 12:407–414.
Javitt DC. 2007. Glutamate and schizophrenia: phencyclidine, N-methyl-D-aspartate receptors, and dopamine-glutamate interactions. Int Rev Neurobiol. 78:69–108.
Javitt DC. 2010. Glutamatergic theories of schizophrenia. Isr J Psychiatry Relat Sci. 47:4–16.
Jedema HP, Moghddam B. 1996. Characterization of excitatory amino acid modulation of dopamine release in the prefrontal cortex of conscious rats. J Neurochem. 66:1448–1453.
Kawahara Y, Kawahara H, Westerink BH. 2002. Hypotension-induced dopamine release in prefrontal cortex is mediated by local glutamatergic projections at the level of nerve terminals. J Neurochem. 81:285–291.
Kessler J, Markowitsch HJ. 1981. Delayed-alternation performance after kainic acid lesions of the thalamic mediodorsal nucleus and the ventral tegmental area in the rat. Behav Brain Res. 3:125–130.
Ko YH, Jung SW, Joe SH, Lee CH, Jung HG, Jung IK, Kim SH, Lee MS. 2007. Association between serum testosterone levels and the severity of negative symptoms in male patients with chronic schizophrenia. Psychoneuroendocrinology. 32:385–391.
Ko YH, Lew YM, Jung SW, Joe SH, Lee CH, Jung HG, Lee MS. 2008. Short-term testosterone augmentation in male schizophrenics: a randomized, double-blind, placebo-controlled trial. J Clin Psychopharmacol. 28:375–383.
Kritzer M. 2004. The distribution of immunoreactivity for intracellular androgen receptors in the cerebral cortex of hormonally intact adult male and female rats: localization in pyramidal neurons making corticocortical connections. Cereb Cortex. 14:268–280.
Kritzer MF. 1997. Selective colocalization of immunoreactivity for intracellular gonadal hormone receptors and tyrosine hydroxylase in the ventral tegmental area, substantia nigra, and retrorubral fields in the rat. J Comp Neurol. 379:247–260.
Kritzer MF. 2000. Effects of acute and chronic gonadectomy on the catecholamine innervation of the cerebral cortex in adult male rats: insensitivity of axons immunoreactive for dopamine-beta-hydroxylase to gonadal steroids, and differential sensitivity of axons immunoreactive for tyrosine hydroxylase to ovarian and testicular hormones. J Comp Neurol. 427:617–633.
Kritzer MF. 2003. Long-term gonadectomy affects the density of tyrosine hydroxylase- but not dopamine-beta-hydroxylase-, choline acetyltransferase- or serotonin-immunoreactive axons in the medial prefrontal cortices of adult male rats. Cereb Cortex. 13:282–296.
Kritzer MF. 2006. Regional, laminar and cellular distribution of immunoreactivity for ERbeta in the cerebral cortex of hormonally intact, postnatally developing male and female rats. Cereb Cortex. 16:1181–1192.
Kritzer MF, Adler A, Marotta J, Smirlis T. 1999. Regionally selective effects of gonadectomy on cortical catecholamine innervation in adult male rats are most disruptive to afferents in prefrontal cortex. Cereb Cortex. 9:507–518.
Kritzer MF, Brewer A, Montalmant F, Davenport M, Robinson JK. 2007. Effects of gonadectomy on performance in operant tasks measuring prefrontal cortical function in adult male rats. Horm Behav. 51:183–194.
Kritzer MF, Creutz LM. 2008. Region and sex differences in constituent dopamine neurons and immunoreactivity for intracellular estrogen and androgen receptors in mesocortical projections in rats. J Neurosci. 28:9525–9535.

Kritzer MF, McLaughlin PJ, Smirlis T, Robinson JK. 2001. Gonadectomy impairs T-maze acquisition in adult male rats. Horm Behav. 39:167–174.
Kus L, Handa RJ, Hautman JM, Beitz AJ. 1995. Castration increases [125I]MK801 binding in the hippocampus of male rats. Brain Res. 683:270–274.
Lee HK, Takamiya K, He K, Song L, Huganir RL. 2010. Specific roles of AMPA receptor subunit GluR1 (GluA1) phosphorylation sites in regulating synaptic plasticity in the CA1 region of hippocampus. J Neurophysiol. 103:479–489.
Lee HK, Takamiya K, Kameyama K, He K, Yu S, Rossetti L, Wilen D, Huganir RL. 2007. Identification and characterization of a novel phosphorylation site on the GluR1 subunit of AMPA receptors. Mol Cell Neurosci. 36:86–94.
Lewis DA, Moghaddam B. 2006. Cognitive dysfunction in schizophrenia: convergence of gamma-aminobutyric acid and glutamate alterations. Arch Neurol. 63:1372–1376.
Livingstone PD, Dickinson JA, Srinivasan J, Kew JN, Wonnacott S. 2010. Glutamate-dopamine crosstalk in the rat prefrontal cortex is modulated by Alpha7 nicotinic receptors and potentiated by PNU-120596. J Mol Neurosci. 40:172–176.
Lodge DJ. 2011. The medial prefrontal and orbitofrontal cortices differentially regulate dopamine system function. Neuropsychopharmacology. 36:1227–1236.
Lu WY, Jackson MF, Bai D, Orser BA, MacDonald JF. 2000. In CA1 pyramidal neurons of the hippocampus protein kinase C regulates calcium-dependent inactivation of NMDA receptors. J Neurosci. 20:4452–4461.
Luine VN. 2008. Sex steroids and cognitive function. J Neuroendocrinol. 20:866–872.
Marek GJ, Behl B, Bespalov AY, Gross G, Lee Y, Schoemaker H. 2010. Glutamatergic (N-methyl-D-aspartate receptor) hypofrontality in schizophrenia: too little juice or a miswired brain? Mol Pharmacol. 77:317–326.
McEwen B. 2002. Estrogen actions throughout the brain. Recent Prog Horm Res. 57:357–384.
McEwen BS. 1996. Gonadal and adrenal steroids regulate neurochemical and structural plasticity of the hippocampus via cellular mechanisms involving NMDA receptors. Cell Mol Neurobiol. 16:103–116.
Moghaddam B. 2003. Bringing order to the glutamate chaos in schizophrenia. Neuron. 40:881–884.
Moghaddam B, Adams B, Verma A, Daly D. 1997. Activation of glutamatergic neurotransmission by ketamine: a novel step in the pathway from NMDA receptor blockade to dopaminergic and cognitive disruptions associated with the prefrontal cortex. J Neurosci. 17:2921–2927.
Morrow BA, Roth RH, Elsworth JD. 2000. TMT, a predator odor, elevates mesoprefrontal dopamine metabolic activity and disrupts short-term working memory in the rat. Brain Res Bull. 52:519–523.
Murphy BL, Arnsten AF, Goldman-Rakic PS, Roth RH. 1996. Increased dopamine turnover in the prefrontal cortex impairs spatial working memory performance in rats and monkeys. Proc Natl Acad Sci U S A. 93:1325–1329.
Nelson EC, Cambio AJ, Yang JC, Lara PN, Jr., Evans CP. 2007. Biologic agents as adjunctive therapy for prostate cancer: a rationale for use with androgen deprivation. Nat Clin Pract Urol. 4:82–94.
Nguyen TV, Yao M, Pike CJ. 2009. Dihydrotestosterone activates CREB signaling in cultured hippocampal neurons. Brain Res. 1298:1–12.
Nunez JL, Huppenbauer CB, McAbee MD, Juraska JM, DonCarlos LL. 2003. Androgen receptor expression in the developing male and female rat visual and prefrontal cortex. J Neurobiol. 56:293–302.
Overton PG, Clark D. 1997. Burst firing in midbrain dopaminergic neurons. Brain Res Brain Res Rev. 25:312–334.
Overton PG, Tong ZY, Clark D. 1996. A pharmacological analysis of the burst events induced in midbrain dopaminergic neurons by electrical stimulation of the prefrontal cortex in the rat. J Neural Transm. 103:523–540.
Patwardhan AJ, Eliez S, Bender B, Linden MG, Reiss AL. 2000. Brain morphology in Klinefelter syndrome: extra X chromosome and testosterone supplementation. Neurology. 54:2218–2223.
Paxinos G, Watson C. 1998. The Rat Brain in Stereotaxic Coordinates, New York: Academic Press, Spiral Bound.
Phillipson OT. 1978. Afferent projections to A10 dopaminergic neurones in the rat as shown by the retrograde transport of horseradisd peroxidase. Neurosci Lett. 9:353–359.
Pratt JA, Winchester C, Egerton A, Cochran SM, Morris BJ. 2008. Modelling prefrontal cortex deficits in schizophrenia: implications for treatment. Br J Pharmacol. 153(Suppl 1):S465–S470.
Ramtekkar UP, Reiersen AM, Todorov AA, Todd RD. 2010. Sex and age differences in attention-deficit/hyperactivity disorder symptoms and diagnoses: implications for DSM-V and ICD-11. J Am Acad Child Adolesc Psychiatry. 49:217–228. e211–e213.
Rodvelt KR, Schachtman TR, Kracke GR, Miller DK. 2008. NMDA receptor blockade augmented nicotine-evoked dopamine release from rat prefrontal cortex slices. Neurosci Lett. 440:319–322.
Rucklidge JJ. 2008. Gender differences in ADHD: implications for psychosocial treatments. Expert Rev Neurother. 8:643–655.
Sandstrom NJ, Kim JH, Wasserman MA. 2006. Testosterone modulates performance on a spatial working memory task in male rats. Horm Behav. 50:18–26.
Schoepp DD, Lodge D, Bleakman D, Leander JD, Tizzano JP, Wright RA, Palmer AJ, Salhoff CR, Ornstein PL. 1995. In vitro and in vivo antagonism of AMPA receptor activation by (3S, 4aR, 6R, 8aR)-6-[2-(1(2)H-tetrazole-5-yl) ethyl] decahydroisoquinoline-3-carboxylic acid. Neuropharmacology. 34:1159–1168.
Schultz W. 1998. Predictive reward signal of dopamine neurons. J Neurophysiol. 80:1–27.
Scott L, Aperia A. 2009. Interaction between N-methyl-D-aspartic acid receptors and D1 dopamine receptors: an important mechanism for brain plasticity. Neuroscience. 158:62–66.
Seeman P. 2009. Glutamate and dopamine components in schizophrenia. J Psychiatry Neurosci. 34:143–149.
Sesack SR, Carr DB. 2002. Selective prefrontal cortex inputs to dopamine cells: implications for schizophrenia. Physiol Behav. 77:513–517.
Sesack SR, Carr DB, Omelchenko N, Pinto A. 2003. Anatomical substrates for glutamate-dopamine interactions: evidence for specificity of connections and extrasynaptic actions. Ann N Y Acad Sci. 1003:36–52.
Shirayama Y, Hashimoto K, Suzuki Y, Higuchi T. 2002. Correlation of plasma neurosteroid levels to the severity of negative symptoms in male patients with schizophrenia. Schizophr Res. 58:69–74.
Simerly RB, Chang C, Muramatsu M, Swanson LW. 1990. Distribution of androgen and estrogen receptor mRNA-containing cells in the rat brain: an in situ hybridization study. J Comp Neurol. 294:76–95.
Smith CC, McMahon LL. 2005. Estrogen-induced increase in the magnitude of long-term potentiation occurs only when the ratio of NMDA transmission to AMPA transmission is increased. J Neurosci. 25:7780–7791.
Smith CC, Vedder LC, McMahon LL. 2009. Estradiol and the relationship between dendritic spines, NR2B containing NMDA receptors, and the magnitude of long-term potentiation at hippocampal CA3-CA1 synapses. Psychoneuroendocrinology. 34(Suppl 1):S130–S142.
Stam CJ, de Bruin JP, van Haelst AM, van der Gugten J, Kalsbeek A. 1989. Influence of the mesocortical dopaminergic system on activity, food hoarding, social-agonistic behavior, and spatial delayed alternation in male rats. Behav Neurosci. 103:24–35.
Strous RD, Maayan R, Lapidus R, Stryjer R, Lustig M, Kotler M, Weizman A. 2003. Dehydroepiandrosterone augmentation in the management of negative, depressive, and anxiety symptoms in schizophrenia. Arch Gen Psychiatry. 60:133–141.
Svensson TH, Tung CS. 1989. Local cooling of pre-frontal cortex induces pacemaker-like firing of dopamine neurons in rat ventral tegmental area in vivo. Acta Physiol Scand. 136:135–136.
Taherianfard M, Shariaty M. 2004. Evaluation of serum steroid hormones in schizophrenic patients. Indian J Med Sci. 58:3–9.
Takahata R, Moghaddam B. 1998. Glutamatergic regulation of basal and stimulus-activated dopamine release in the prefrontal cortex. J Neurochem. 71:1443–1449.
Tassin JP, Stinus L, Simon H, Blanc G, Thierry AM, Le Moal M, Cardo B, Glowinski J. 1978. Relationship between the locomotor hyperactivity

induced by A10 lesions and the destruction of the fronto-cortical dopaminergic innervation in the rat. Brain Res. 141:267–281.
Tong ZY, Overton PG, Clark D. 1996a. Antagonism of NMDA receptors but not AMPA/kainate receptors blocks bursting in dopaminergic neurons induced by electrical stimulation of the prefrontal cortex. J Neural Transm. 103:889–904.
Tong ZY, Overton PG, Clark D. 1996b. Stimulation of the prefrontal cortex in the rat induces patterns of activity in midbrain dopaminergic neurons which resemble natural burst events. Synapse. 22:195–208.
van Haaren F, van Hest A, Heinsbroek RP. 1990. Behavioral differences between male and female rats: effects of gonadal hormones on learning and memory. Neurosci Biobehav Rev. 14:23–33.
Verma A, Moghaddam B. 1996. NMDA receptor antagonists impair prefrontal cortex function as assessed via spatial delayed alternation performance in rats: modulation by dopamine. J Neurosci. 16:373–379.
Wainman P, Shipounoff GC. 1941. The effects of castration and testosterone on the striated perineal musculature in the rat. J Endocrinol. 29:975.
Westerink BH, Enrico P, Feimann J, De Vries JB. 1998. The pharmacology of mesocortical dopamine neurons: a dual-probe microdialysis study in the ventral tegmental area and prefrontal cortex of the rat brain. J Pharmacol Exp Ther. 285:143–154.
Winterer G, Weinberger DR. 2004. Genes, dopamine and cortical signal-to-noise ratio in schizophrenia. Trends Neurosci. 27:683–690.
Woolley CS. 1998. Estrogen-mediated structural and functional synaptic plasticity in the female rat hippocampus. Horm Behav. 34:140–148.
Young LA, Neiss MB, Samuels MH, Roselli CE, Janowsky JS. 2010. Cognition is not modified by large but temporary changes in sex hormones in men. J Clin Endocrinol Metab. 95:280–288.
Zahn-Waxler C, Shirtcliff EA, Marceau K. 2008. Disorders of childhood and adolescence: gender and psychopathology. Annu Rev Clin Psychol. 4:275–303.
Zahrt J, Taylor JR, Mathew RG, Arnsten AF. 1997. Supranormal stimulation of D1 dopamine receptors in the rodent prefrontal cortex impairs spatial working memory performance. J Neurosci. 17:8528–8535.